Molecular Cancer Research

Cancer Cell Dependence on Unsaturated Fatty Acids Implicates Stearoyl-CoA Desaturase as a Target for Cancer Therapy

Urvashi V. Roongta[1], Jonathan G. Pabalan[1], Xinyu Wang[1], Rolf-Peter Ryseck[1], Joseph Fargnoli[1], Benjamin J. Henley[1], Wen-Pin Yang[2], Jun Zhu[2], Malavi T. Madireddi[3], R. Michael Lawrence[4], Tai W. Wong[1], and Brent A. Rupnow[1]

Abstract

Emerging literature suggests that metabolic pathways play an important role in the maintenance and progression of human cancers. In particular, recent studies have implicated lipid biosynthesis and desaturation as a requirement for tumor cell survival. In the studies reported here, we aimed to understand whether tumor cells require the activity of either human isoform of stearoyl-CoA-desaturase (SCD1 or SCD5) for survival. Inhibition of SCD1 by siRNA or a small molecule antagonist results in strong induction of apoptosis and growth inhibition, when tumor cells are cultured in reduced (2%) serum conditions, but has little impact on cells cultured in 10% serum. Depletion of SCD5 had minimal effects on cell growth or apoptosis. Consistent with the observed dependence on SCD1, but not SCD5, levels of SCD1 protein increased in response to decreasing serum levels. Both induction of SCD1 protein and sensitivity to growth inhibition by SCD1 inhibition could be reversed by supplementing growth media with unsaturated fatty acids, the product of the enzymatic reaction catalyzed by SCD1. Transcription profiling of cells treated with an SCD inhibitor revealed strong induction of markers of endoplasmic reticulum stress. Underscoring its importance in cancer, SCD1 protein was found to be highly expressed in a large percentage of human cancer specimens. SCD inhibition resulted in tumor growth delay in a human gastric cancer xenograft model. Altogether, these results suggest that desaturated fatty acids are required for tumor cell survival and that SCD may represent a viable target for the development of novel agents for cancer therapy. *Mol Cancer Res; 9(11); 1551–61. ©2011 AACR.*

Introduction

Stearoyl-CoA desaturase (SCD) enzymes catalyze the conversion of saturated fatty acids (SFA) to Δ-9 monounsaturated fatty acids (MUFA). These enzymes preferentially convert stearic acid (C18:0) to oleic acid (C18:1) and palmitic acid (C16:0) to palmitoleic acid (C16:1; ref. 1). In mammals, the most extensively studied SCDs are those from the mouse in which 4 isoforms (SCD1–4) are known to exist (reviewed in ref. 2). Of the 2 human SCD genes, *SCD1* and *SCD5*, only human *SCD1* has been extensively studied and is the nearest ortholog of the 4 murine enzymes. Much less is known about human SCD5, however it seems, by sequence comparison, to be divergent from the 4 rodent SCD isoforms (3).

The products of SCD enzymes, oleic and palmitoleic acids, are the most abundant MUFAs and represent important precursors for the formation of complex lipids including phospholipids, triglycerides, cholesterol esters, wax esters, and diacylglycerols. Hence, the activity of SCD enzymes is likely to have wide-ranging effects on cellular membrane physiology, energy storage, and signaling, as well as broad effects on animal physiology. Recently, a number of reports have implicated SCD1 expression and activity in the pathogenesis of cancer (for review see ref. 4). Human SCD1 mRNA was found to be overexpressed in a variety of human cancers, including colon, esophageal, and hepatocellular carcinomas relative to the corresponding normal tissues (5). In addition, SCD1 levels were found to be elevated in mice and rats that are genetically predisposed to develop certain cancers (6). SCD1 levels were also observed to be upregulated in transformed cells. Both expression and activity of human SCD1 were found to increase in human fibroblasts upon transformation by SV40 (7); the same authors subsequently showed that reducing SCD1 levels in SV40-transformed fibroblasts using antisense mRNA expression resulted in reduced proliferation and a diminished capacity for anchorage-independent growth (8). Conversely,

Authors' Affiliations: [1]Oncology Drug Discovery, [2]Applied Biotechnology, [3]Metabolic Disease Drug Discovery, and [4]Discovery Chemistry, Bristol-Myers Squibb R&D, Princeton, New Jersey

Note: Supplementary data for this article are available at Molecular Cancer Research Online (http://mcr.aacrjournals.org/).

Corresponding Author: Brent A. Rupnow, Department of Oncology Drug Discovery, Bristol-Myers Squibb R&D, PO Box 4000, Princeton, NJ 08543. Phone: 609-252-4269; Fax: 609-252-6051; E-mail: brent.rupnow@bms.com

doi: 10.1158/1541-7786.MCR-11-0126

it was recently reported that SCD1 levels decreased in fibroblasts undergoing senescence compared with low passage, rapidly proliferating fibroblasts (9, 10).

As with engineered fibroblasts, human cancer cell lines have been reported to depend on the expression of SCD1 for proliferation and survival. Scaglia and Igal showed that even modest suppression of SCD1 levels and activity in A549 lung cancer cells by stable expression of SCD1-targeted antisense RNA resulted in reduced proliferation rate, a reduced capacity for growth in soft agar, and delayed growth of xenografts in nude mice (10). The reduction in tumorigenic activity in these cell lines with reduced SCD1 activity correlated with reduced levels of MUFAs and has been linked to effects on the AKT and AMPK signaling pathways (10, 11). Independently, Morgan-Lappe and colleagues identified SCD1 in an RNA interference (RNAi) screen for proteins required for maintaining tumor cell survival (12). The authors went on to show that the extent of depletion of SCD1 protein levels in H1299 lung cancer cells correlated strongly with the degree of reduction in cell survival and that reduced survival in SCD1-depleted cells resulted from caspase-3–dependent apoptosis. Recently, 2 reports have shown that pharmacologic inhibitors of SCD1 cause diminished tumor cell growth in prostate and lung cancer models (13, 14).

Given these preliminary implications of SCD1 in the growth and survival of cancer cells, we set out to further characterize the level of tumor cell dependence on cellular lipid desaturation and to determine whether SCD1 and/or SCD5 might represent a viable drug target for pharmacologic intervention in human cancer.

The studies reported here show, for the first time, that tumor cells are highly dependent on MUFA for proliferation and that in the absence of an exogenous MUFA source, they become entirely dependent on the activity of SCD1. Furthermore, we show that levels of SCD1 protein are tightly regulated by exogenous MUFA availability and that high expression of SCD1 correlates with the dependence of tumor cells upon its activity. Finally, high SCD1 protein was commonly found in a variety of human cancers, and pharmacologic inhibition of SCD1 in a high expressing xenograft resulted in significant antitumor effects. Together, these results strongly suggest that SCD1 represents a viable target for the development of novel anticancer agents.

Materials and Methods

Cell lines and culture conditions

A549, H1299, and FaDu human cancer cell lines were acquired from the American Type Culture Collection. Cells were maintained in Dulbecco's modified Eagle's medium containing high glucose and L-glutamine (Invitrogen) supplemented with fetal bovine serum (FBS; Invitrogen) or charcoal-stripped FBS (CS-FBS; Innovative Research). Cell cultures were incubated at 37°C, 5% CO_2, and 100% humidity. Where indicated, cultures were supplemented with BSA-conjugated fatty acids. BSA-conjugated oleic acid (catalog #O3008) and fatty acid–free bovine serum albumin (BSA, catalog #A8806) were purchased from Sigma-Aldrich.

RNA interference

siRNA duplexes targeting human SCD1 (catalog #J-005061-07, J-005061-08, and J-005061-10) and human SCD5 (catalog #J-008416-06, J-008416-07, and J-008416-08) were obtained from Dharmacon RNAi Technologies. RISC free siRNA (catalog #D-001220-01) and a custom synthesized siRNA designed against the firefly luciferase mRNA sequence (5′- GGGACGAAGACGAACACUUC-3′) were used as negative controls. Cells were transfected using Lipofectamine 2000 (Invitrogen) according to the manufacturer's protocol. siRNAs were delivered to cells at a final concentration of 20 nmol/L.

Antibodies and immunoblotting

Antibodies specific for human SCD1 and human SCD5 were raised by immunizing rabbits with fusion proteins containing an SCD1-specific peptide sequence (PPSRVLQNGGDKLETMPLYLEDDIRPDIKDD) and an SCD5-specific peptide sequence (MPGPATDAG-KIPFCDAKEEIRAGLESSEGG). To generate the fusion protein antigens, oligonucleotides encoding the SCD1 and SCD5 peptides were cloned into the pEX34a bacterial expression vector, and fusion proteins were expressed in *Escherichia coli* K537 as described (15). Specificity of the antisera was confirmed by testing against the full-length proteins using immunoprecipitation and Western blotting techniques. Mouse anti-actin antibody (catalog #MAB1501R) was purchased from Chemicon. Labeled sheep anti-Rabbit IgG (catalog #611-632-122) was purchased from Rockland Immunochemicals. Labeled goat anti-mouse IgG (catalog #A21057) was purchased from Invitrogen. Anti-p85 cleaved PARP polyclonal antibody (catalog #G7341) was purchased from Promega. Fluorescein isothiocyanate (FITC)-conjugated anti-rabbit antibody (catalog #554020) was acquired from BD Biosciences.

Following siRNA or compound treatments, cells were lysed by scraping into radioimmunoprecipitation assay buffer (catalog #R0278; Sigma-Aldrich) containing Protease Inhibitor Cocktail (catalog #P8340; Sigma-Aldrich). Protein concentrations were determined and Western blotting was done using standard procedures. Blots were probed for 2 hours with the indicated primary antibodies and developed using infrared dye–labeled secondary antibodies. Blot images were captured using a Li-Cor Odyssey Infrared Imaging System.

Quantitation of apoptosis

Induction of apoptosis was assessed by measuring the number of cells producing the p85 fragment of cleaved PARP by flow cytometry as previously described (16). Anti-p85–cleaved PARP polyclonal antibody was used at a 1:200 dilution from the manufacturer's stock (catalog #G7341; Promega). Flow cytometry to determine DNA content (PI fluorescence intensity) and PARP cleavage (FITC fluorescence) was done on a Becton Dickinson FACSCanto with Diva 6.1.1 software, and the data was analyzed using the FlowJo 8.5.3 software package. Data are

presented as the fold increase in the percentage of apoptotic cells relative to Luc-negative control siRNA-transfected cells.

SCD activity determination

In vitro SCD1 activity was determined using a modified version of the assay described by Obukowicz and colleagues (17). Microsomes were prepared from Sf9 insect cells coexpressing recombinant human SCD1 and Cytochrome b5/b5R. Microsome mixture, containing 1 μg of baculovirus expressed human SCD1 in 100 mmol/L potassium phosphate buffer (pH 7.4), and compound in dimethyl sulfoxide (DMSO) was added to each well and preincubated for 10 minutes. The reaction was initiated with the addition of the substrate mixture which contained the following: 5 μmol/L Stearoyl-CoA (Sigma Aldrich), 0.25 μmol/L Stearoyl [9,10-^{3}H] CoA (catalog #ART 0390; American Radiolabeled Chemicals), 5 mmol/L NADH (Roche) in 100 mmol/L potassium phosphate buffer (pH 7.4). After a 10-minute incubation at room temperature, the reaction was stopped by the addition of 50% trichloroacetic acid and mixed for 5 minutes on a shaker. The reaction mixture was then transferred to a 96-well Millipore Multiscreen Plate (Millipore; catalog# MSGVN22) and 125 mg/mL charcoal was added to each well. Plates were shaken for 10 minutes and [^{3}H]-H_2O was separated from the reaction by filtering into a Isoplate collection plate (Wallac–PerkinElmer; catalog# 1450–514) preloaded with OptiPhase Supermix scintillation fluid (PerkinElmer; catalog # 1200–439). Radioactivity was counted on a Wallac Microbeta TriLux counter. Cellular SCD1 activity was determined using the method described by Dillon and colleagues (18). D7-stearic acid (Octadecanoic-16,16,17,17,18,18,18-d_7 Acid, catalog # D-6777) was obtained from CDN Isotopes (Pointe-Claire). For both *in vitro* and cellular assays, SCD1 activity was calculated relative to control reactions containing DMSO only.

Cell growth assays

For A939572 IC_{50} determinations, cells were plated in 96-well plates (2,000–4,000 cells per well). Cells were treated with A939572 at concentrations ranging from 1 nmol/L to 10 μmol/L or DMSO only control. After 72 hours of incubation of cells with compound, cell viability was measured using the CellTiter 96 AQ_{ueous} Non-Radioactive Cell Proliferation Assay (MTS; Promega; catalog #G5421) according to the manufacturer's protocol. Percent inhibition for wells treated with A939572 was determined relative to wells treated with DMSO alone.

Cell growth kinetics in both 10% and 2% FBS, with and without 100 nmol/L A939572 was assessed by time-lapse microscopy using an IncuCyte Imaging System (Essen Bioscience). Photomicrographs were captured every 12 hours. From these photomicrographs, the IncuCyte Imaging system calculated the average percent confluence for each treatment, and data are reported over a 5-day period.

Transcription profiling

H1299 cells were seeded on 6-well plates (25,000 to 30,000 cells per well) in media containing 2% or 10% FBS overnight. Cells were then treated with vehicle (DMSO) or A939572 at the indicated concentration. After 24 hours, cells were lysed with Nucleic Acid Purification Lysis Solution (Applied Biosystems) and total RNA was prepared using the Prism 6100 instrument (Applied Biosystems). The total RNA was then treated with DNase I in the presence of RNase Inhibitor for 10 minutes and purified with magnetic beads using BioSprint 96 (Qiagen). Complementary RNA preparation and hybridization onto U133A arrays was done according to manufacturer's protocols (Affymetrix). The hybridization intensity was derived from Affymetrix MAS5.0 algorithm with quantile normalization, obtained from www.bioconductor.org. Probe sets without 2 data points with intensity greater than 100 were removed from further analysis. Significantly changed genes were determined on the basis of a minimum fold change (mean normalized expression value in A939572-treated sample divided by mean normalized expression value in DMSO-treated samples) of 1.5 and *P* value from *t* test of less than 0.005. Taking multiple test correction into consideration, the false discovery rate using these criteria is 0.25. Table 2 lists all significantly altered genes with fold changes greater than 2.0.

SCD1 immunohistochemistry

A tissue microarray (TMA) of formalin fixed, paraffin-embedded (FFPE) tumor tissues was prepared by Asterand UK Ltd. The TMA contained 11 tissue types including breast, colon, lymphoid, and prostate (8 tumor and 2 normal samples of each), gastric, ovary, brain, kidney, liver, and skin (4 tumor and 2 normal samples of each), and lung (8 non–small cell tumor and 4 small cell tumor samples, and 4 normal samples). Sections (4 μm) of the FFPE TMA were stained using standard immunohistochemistry (IHC) techniques. Rabbit polyclonal anti-human SCD1 antibody diluted in Background Reducing Diluent (catalog #S3022; Dako) was applied at a concentration of 1 μg/mL. The negative control sections were incubated with a nonimmune rabbit IgG antibody (catalog #X0936; Dako) at 1 μg/mL. Antibody amplification and visualization steps were carried out using the CSA II kit (catalog #K1501; Dako). Following chromagenesis, the sections were counterstained with haematoxylin, dehydrated and coverslipped under DePeX. Stained sections were analyzed and suitable digital images captured, using an Olympus BX51 microscope with a Leica DFC290 camera attached. Immunohistochemical analysis of human primary xenograft heterotransplants was done at Crown Bioscience Inc. following the same protocol.

In vivo pharmacology

Primary human cancer xenograft studies were done at Crown Bioscience Inc. The GA16 primary xenograft, derived from a gastric carcinoma patient, was implanted and then maintained subcutaneously in nude mice. GA016 tumors grown to 500 to 700 mm^3 were harvested for tumor inoculation. Tumors were minced into approximately 30 mm^3 fragments. One tumor fragment was subcutaneously implanted into the right rear flank of each Balb/c nude

mouse. Mice were maintained on Teklad Global 18% Protein Rodent Diet (catalog #2018; Teklad Diets). For antitumor efficacy studies, the GA16 tumor implant was passage number 6 after the derivation of the xenograft from the original surgical specimen. Fourteen days after inoculation, tumors reached an average size of 150 mm^3. At that time, tumors were measured and assigned randomly to 2 groups of 8 mice each, such that the mean tumor volume for each group was roughly equal. On day 15, mice began treatment with vehicle [50% v/v Polyethylene Glycol (PEG) 400, 20% v/v Propylene Glycol (PG), 20% v/v Vitamin E TPGS (d-alpha tocopheryl polyethylene glycol 1000 succinate), 5% v/v ethanol, 5% w/v polyvinylpyrrolidone (K12 PVP)], or 100 mg/kg A939572 in vehicle. Mice received vehicle or compound via oral gavage twice daily for 21 days. Tumor volumes were calculated from direct tumor measurements every 3 to 4 days using the formula: 1/2 [length × $(width)^2$]. Animal body weights were determined on the same days that tumor measurements were taken.

Results

SCD1 depletion by siRNA results in serum-dependent reduction in cell viability

siRNA knockdown was done to assess the importance of SCD1 and SCD5 to proliferation and survival of human cancer cells. Cell lines that express both SCD isoforms were transfected with 3 siRNAs specific for each target and protein levels were determined at 48 hours after transfection (Fig. 1A). siRNA modified to block binding to the RISC complex (RISC free) and siRNA designed to target firefly luciferase (Luc) were included as negative controls. Transfection of cells with SCD1 and SCD5 siRNAs resulted in specific knockdown of the target proteins. Cells transfected with control siRNAs showed no alteration in SCD1 or SCD5 protein levels relative to untransfected cells.

The effects of SCD1 or SCD5 depletion on the induction of apoptosis was determined by measuring the production of the p85 fragment of cleaved PARP using flow cytometry (Fig. 1B). When cells were grown in 10% FBS, there was little induction of apoptosis when SCD1 was depleted. However, in cells that were transfected with SCD1-targeting siRNAs cultured in reduced serum conditions (2% FBS), substantial apoptosis induction was observed. Under these conditions, the relative extent of apoptosis induction between the 3 SCD1-targeting siRNAs correlated strongly with the degree of SCD1 depletion. In contrast to SCD1, depletion of SCD5 did not result in substantial apoptosis of any cell line tested regardless of serum concentration.

Pharmacologic inhibition of SCD1 results in serum-dependent reduction in cell proliferation

The results obtained with siRNAs were confirmed using a previously reported inhibitor of SCD1, A939572 (compound 4C in ref. 19). The IC_{50} value for A939572 was determined using a recombinant microsome desaturation assay that measures formation of tritiated water upon desaturation of stearic acid labeled with tritium at C9 and C10 (17, 20, 21). The IC_{50} value for A939572 was found to be 6.3 nmol/L in human SCD1 expressing microsomes. In addition, the IC_{50} value for A939572 was determined in a cellular assay for desaturation index (DI IC_{50}; Fig. 2A; ref. 18). A939572 was found to be equally potent at inhibiting desaturation in a cellular context and in an *in vitro* biochemical reaction. DI IC_{50} in FaDu cells was determined to be approximately 4 nmol/L.

The effect of A939572 on cell proliferation was evaluated in a 72-hour growth inhibition assay. Figure 2B shows concentration response curves for cells treated in 10% or 2% serum conditions. Under 10% serum conditions, the IC_{50} value for growth inhibition of FaDu cells by A939572 was determined to be more than 5 μmol/L, whereas the IC_{50} in 2% serum was 0.029 μmol/L. The effects of A939572 on cell growth kinetics were also determined under both serum culture conditions (Fig. 2C). Culturing cells in 2% serum without compound treatment only slightly slowed their growth kinetics relative to 10% serum concentration. However, in cells grown in 2% FBS, exposure to 100 nmol/L A939572 strongly inhibited proliferation. Conversely, exposure of cells to A939572 in 10% FBS containing media had little effect on the growth of cells over the first 72 hours of growth. However, all 3 cells lines exhibited some growth inhibition between 72 and 120 hours of culture time. This effect was minimal in FaDu, moderate in A549, and more pronounced in H1299 cells.

Serum-derived MUFAs determine expression of SCD1 protein and sensitivity to SCD inhibition

To explore the mechanism underlying the serum-dependent differential sensitivity of cells to inhibition of SCD, the levels of SCD1 and SCD5 were measured in the sensitive (reduced serum) or resistant (normal serum) contexts. Western blotting for SCD1 and SCD5 in the 3 cell lines revealed a marked induction of SCD1 in cells cultured in media containing 2% FBS relative to cells cultured in media containing 10% FBS (Fig 3A). By contrast, SCD5 levels were mostly unchanged by serum concentration.

The only known cellular function of SCD is the production of MUFAs, and the only source of exogenous MUFA under our culture conditions is FBS supplementation. It was therefore hypothesized that the reduced MUFA available to cells grown in media containing 2% FBS (relative to 10% FBS) may be responsible for the induction of SCD1 and the corresponding dependence on this enzyme for proliferation and survival. To test this hypothesis, cells were grown in media supplemented with normal FBS or FBS that had been stripped with charcoal to remove lipids (CS-FBS). Figure 3B shows immunoblot analysis of lysates from H1299 and FaDu cells grown for 1, 2, or 3 days in the presence of 10% FBS, 2% FBS, 10% CS-FBS, or 2% CS-FBS. Under normal growth conditions (media + 10% FBS), SCD1 levels remained low over the course of 3 days. However, in cells grown in reduced serum conditions, SCD1 protein was induced to very high levels within 24 to 48 hours. Conversely, in charcoal-stripped serum, SCD1 protein levels were rapidly induced regardless of the serum concentration.

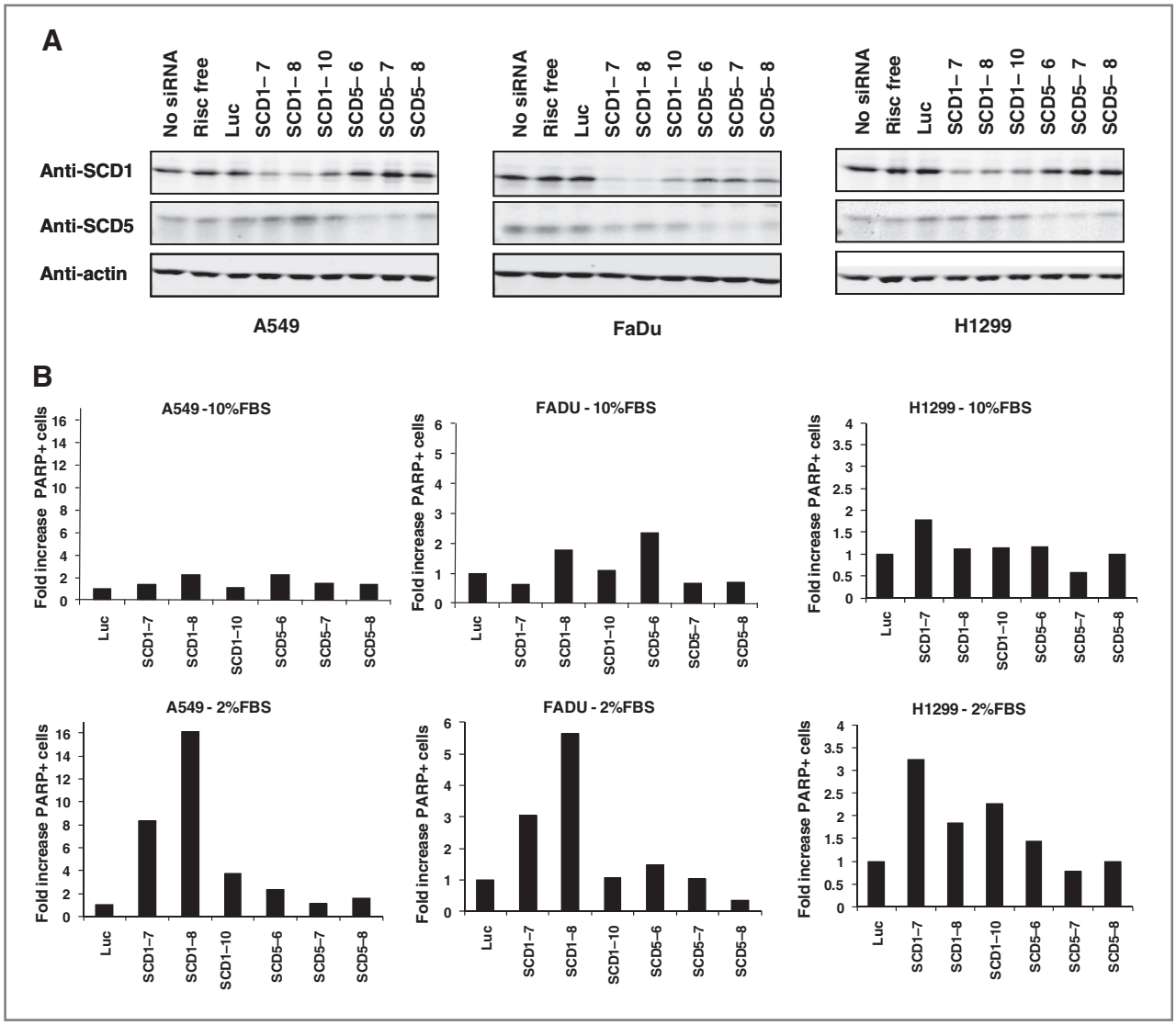

Figure 1. Depletion of SCD1, but not SCD5, induces apoptosis in tumor cells in a manner dependent on serum concentration. A, Western blot analysis of SCD1, SCD5, and actin in A549, FaDu, and H1299 cell lines transfected with siRNAs targeting SCD1 (SCD1-7, SCD1-8, and SCD1-10) or SCD5 (SCD5-5, SCD5-7, and SCD5-8) as well as negative control siRNAs including Luc which is designed to target firefly luciferase and RISC free that is modified to prevent incorporation into the RISC silencing complex. B, apoptosis induced by SCD1 or SCD5 depletion in A549, FaDu, and H1299 cells grown in media containing either 10% FBS or 2% FBS. Apoptosis is expressed as the ratio of the percentage of cells determined to be apoptotic (positive for the p85 fragment of cleaved PARP by flow cytometry) in cultures transfected with siRNAs against the SCD isoforms to the percentage of cells positive for p85 PARP in cells transfected with the Luc-negative control siRNA.

To understand the connection between SCD1 induction in cells grown under reduced or charcoal-stripped serum conditions and sensitivity to SCD1 inhibition, cellular IC_{50} values for growth inhibition by A939572 were determined (Table 1). Cells grown in 10% FBS were refractory to growth inhibition by A939572, whereas cells in reduced serum (2%) or charcoal-stripped serum (both 2% and 10%) were highly sensitive to growth inhibition by the SCD1 inhibitor. Differential sensitivity was observed between cells supplemented with 10% or 2% CS-FBS. This likely reflects an incomplete removal of serum lipids by charcoal stripping. Importantly, for all 4 conditions tested, the relative sensitivity to SCD1 inhibition by A939572 correlated strongly with the relative level of SCD1 induction observed (Fig. 3B and Table 1).

To confirm that the sensitization of cells to SCD1 inhibition by reduced serum is related to limiting availability of unsaturated fatty acids, we tested whether cells could be rescued from sensitivity by the addition of exogenous oleic acid conjugated to bovine serum albumin (BSA-conjugated oleic acid) into the growth media (Fig. 3C). In the absence of BSA or BSA-conjugated oleic acid, A939572 treatment caused dose-dependent inhibition of cell proliferation. Addition of BSA alone did not

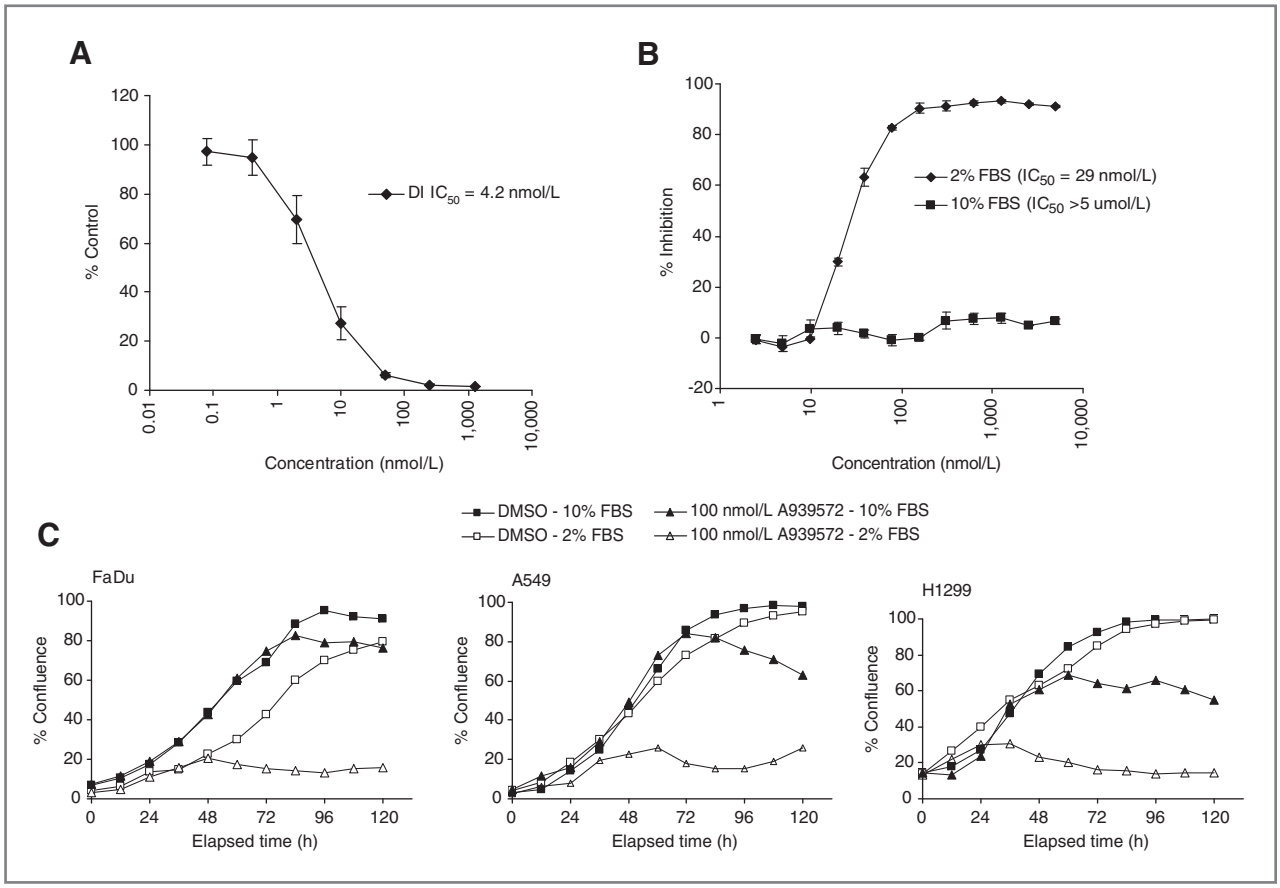

Figure 2. Pharmacologic inhibition of SCD1 potently inhibits proliferation in tumor cells cultured in reduced serum conditions. A, dose-dependent inhibition of SCD1 activity in FaDu cells as determined by mass spectrometric measurement of the conversion of deuterated stearic acid to deuterated oleic acid. Data are presented as the percent of deuterated oleic acid produced in A939572-treated cells relative to DMSO-treated control cells. Data points are the mean of 3 independent replicates at each dose level. Error bars represent SD from the mean. B, percent inhibition of cell viability at varying concentrations of A939572 in FaDu cells relative to DMSO-treated control cells. Data are shown for cells treated for 72 hours in media containing either 10% FBS or 2% FBS. Cell viability was determined using the MTS assay in 3 independent replicates at each dose level. Error bars represent the SD from the mean. C, effects of A939572 treatment on cell growth kinetics for FaDu, A549, and H1299 cells cultured in media containing either 10% FBS or 2% FBS. At 12-hour intervals, the confluence of cells in both media conditions, with and without 100 nmol/L A939572, was determined using the IncuCyte live cell imaging system.

alter the dose response of cells to A939572. However, the addition of BSA-conjugated oleic acid showed a dose-dependent rescue of cell sensitivity to A939572 treatment. Levels of SCD1 protein was also examined in cells supplemented with BSA or conjugated oleic acid (Fig. 3D). The addition of BSA-conjugated oleic acid reduced SCD1 protein levels in a dose-dependent manner relative to supplementation with BSA alone. Extending upon this result, we also tested the effects of supplementing media with other fatty acids, both saturated and unsaturated. Like oleic acid, supplementing growth media with BSA-conjugated palmitoleic acid or linoleic acid protected cells from growth inhibition upon SCD1 inhibition, whereas SFA supplementation with either stearic acid or palmitic acid did not (Supplementary Fig. S1). Furthermore, under these conditions, SFA supplementation did not induce cell killing on its own, nor did it enhance the antiproliferative effect of SCD1 inhibition.

Cell killing by SCD1 inhibition in conditions of limiting MUFA occurs via a mechanism involving the ER stress response

To shed light on the mechanism of cell killing by SCD1 inhibition, H1299 cells were treated with A939572 at 100 nmol/L or DMSO vehicle control under reduced serum conditions, and global transcription profiling was done using Affymetrix microarrays. Analysis of the data revealed 56 statistically significant transcriptional changes ($P < 0.005$ and fold change more than 1.5×), 18 of these changed by more than 2-fold. Table 2 lists those genes whose expression level increased or decreased by more than 2-fold (fold change refers to the relative increase in expression of the mRNA in cells treated with A939572 versus cells treated with DMSO control at the indicated serum concentration). None of the transcriptional changes observed in reduced serum conditions were significantly different in cells treated with A939572 and DMSO under normal serum conditions. The

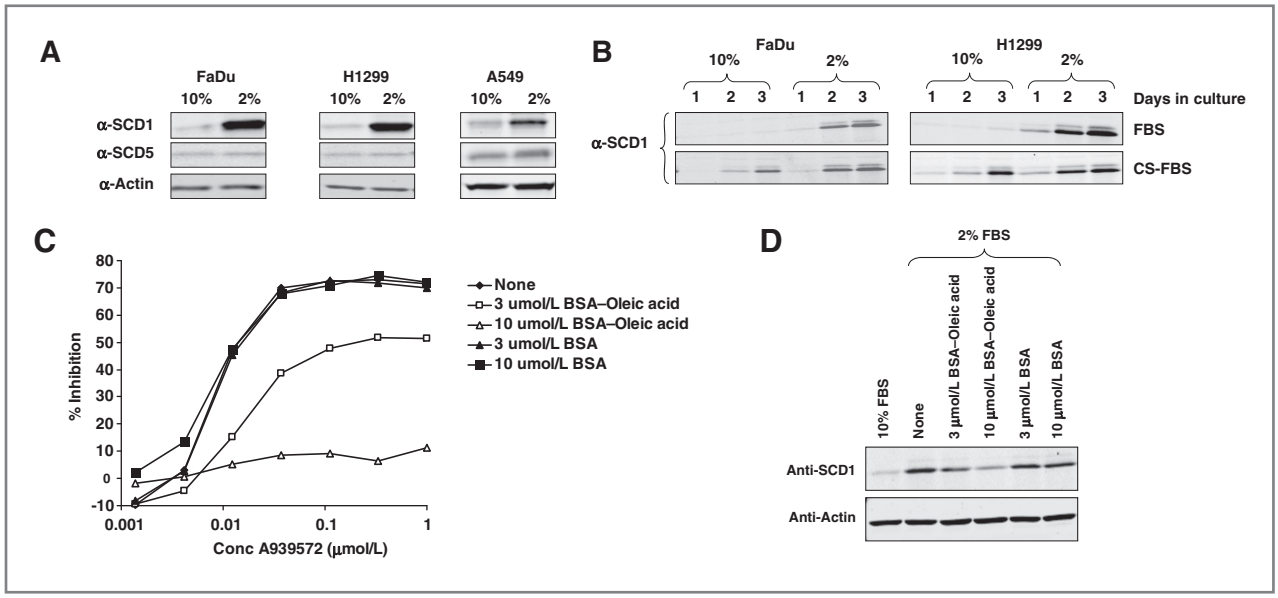

Figure 3. SCD1 protein levels are regulated by serum concentration, predict sensitivity to SCD1 inhibition, and can be rescued by oleic acid supplementation. A, Western blot analysis of SCD1 and SCD5 proteins in FaDu, H1299, and A549 cells cultured for 48 hours in media containing either 10% or 2% FBS. Blots were also probed with actin-specific antibodies to ensure equal loading. B, time-dependent induction of SCD1 in FaDu and H1299 cells cultured in 10% or 2% normal FBS as well as CS-FBS. C, cell growth inhibition by A939572 in FaDu cells cultured for 72 hours in 2% FBS is rescued by addition of BSA-conjugated oleic acid but not by BSA alone. D, Western blot analysis of SCD1 in 10% FBS, 2% FBS, and with supplementation of BSA-conjugated oleic acid or BSA alone shows that SCD1 induction under reduced serum is reduced by BSA–oleic acid supplementation.

most highly induced transcript encodes the C/EBP homologous protein (CHOP, gene symbol *DDIT3*). CHOP, along with other A939572-regulated genes including BiP/GRP78 are among the most well-studied markers of endoplasmic reticulum (ER) stress in mammalian cells (22). Upon review of the literature, we found that half of the 18 genes, including the 5 most highly modulated genes in this study, are implicated in cellular responses to and/or resolution of ER stress (references cited in Table 2). To confirm that the A939572-induced gene expression changes related to ER stress response are specific to SCD1 inhibition, we transfected H1299 cells with siRNA-targeting SCD1 and measured the effect of SCD1 depletion on the levels of mRNA coding for DDIT3, TRIB3, ATF3, and SLC7A11 (Supplementary Fig. S2). Using quantitative real-time PCR, all 4 genes were found to be induced by more than 10-fold in SCD1 (SCD1-7) siRNA-treated cells relative to control (Luc) siRNA–treated cells cultured in media containing 2% FBS. Little or no change in gene expression was observed in the same experiment conducted in cells cultured with 10% FBS.

Table 1. IC_{50} values for inhibition of cell viability by A939572 in FaDu and H1299 cells cultured in 10% or 2% FBS and 10% or 2% CS-FBS

	FaDu IC_{50} (μmol/L)	H1299 IC_{50} (μmol/L)
10% FBS	>10.0	>10.0
2% FBS	0.019	0.057
10% CS-FBS	0.049	0.155
2% CS-FBS	0.012	0.014

SCD1 protein is highly expressed in human cancers

To gain insight into the role of SCD1 in human cancer, IHC was done to detect SCD1 protein levels in human cancer specimens. A paraffin-embedded TMA containing 61 cores from 11 common human cancer subtypes was stained using an antibody specific for human SCD1. The staining of representative tissue cores from 4 tumor types and corresponding normal tissues is shown in Fig. 4. As expected, staining was found predominantly in the perinuclear region of cells staining positive, consistent with the ER localization of SCD1 protein. In many of the tissue cores, variable expression was observed within the tumor ranging from 1+ to 3+ for individual cells (Fig. 4A). Expression of SCD1 was found to be relatively low in the normal tissues examined compared with the corresponding tumor tissue. This is exemplified by the core pictured in Fig. 4B, which contained colon cancer tissue as well as adjacent normal colon epithelium. Whereas normal colon epithelial tissue (red box) stained negative for SCD1 protein, colon cancer tissue (green box) showed high levels of SCD1 staining. Certain normal tissues, including breast and prostate, showed moderate SCD1 protein expression in the glandular epithelium (Fig. 4A). Alveolar macrophages in lung tissue also stained positively for SCD1 expression.

The intensity of staining of each tissue core on the TMA was qualitatively scored using standard pathologic scoring terms (0, 1+, 2+, and 3+) to assess the overall level of

Table 2. Gene expression changes induced by A939572 in H1299 cells under normal and reduced serum concentrations

Gene name (symbol)	Fold change 2% FBS	Fold change 10% FBS	ER stress pathway?
C/EBP homologous protein (*DDIT3*, *CHOP*)	6.66	0.88	Yes (22)
Tribbles homolog 3 (*TRIB3*)	5.45	1.13	Yes (35)
DNA damage inducible transcript 4 (*DDIT4*)	5.05	1.05	Yes (36)
Activating transcription factor 3 (*ATF3*)	4.40	1.12	Yes (37)
Cation transport regulator homolog 1 (*CHAC1*)	3.88	1.24	
Solute carrier 7A11 (*SLC7A11*, *xCT*)	3.80	0.90	Yes (38)
Homocysteine inducible, ER stress inducible, ubiquitin-like domain member 1 (*HERPUD1*)	3.74	0.99	Yes (39)
Phosphoenolpyruvate carboxykinase 2 (*PCK2*)	3.58	0.97	
Jun D proto-oncogene (*JUND*)	2.95	0.98	
Class B basic helix-loop-helix protein 2 (*BHLHB2*)	2.57	1.40	
Asparagine synthetase (*ASNS*)	2.49	1.10	Yes (40)
Stanniocalcin 2 (*STC2*)	2.37	1.78	Yes (41)
Phosphoserine aminotransferase 1 (*PSAT1*)	2.21	0.94	
Heat shock 70kDa protein 5 (*HSPA5*, *BiP*, *GRP78*)	2.19	1.15	Yes (42)
Serine palmitoyltransferase, long chain 2 (*SPTLC2*)	2.18	0.92	
Tripartite motif-containing 16 (*TRIM16*)	2.05	1.02	
F-box and WD40 repeat domain 7 (*FBXW7*)	2.02	0.71	
Heparan sulfate proteoglycan 2 (*HSPG2*)	0.22	0.84	

expression of the target protein in the various tissues. SCD1 expression was detectable in greater than 75% of tumors tested (Supplementary Table S1). Furthermore, greater than 50% of tumors showed 2+ staining or higher.

Inhibition of SCD1 results in tumor growth inhibition

Given the potent antiproliferative activity of A939572 in cultured cells that expressed high levels of SCD1 protein, we set out to evaluate the antitumor activity of SCD1 inhibition. We reasoned that high expression of SCD1 would predict sensitivity of tumors to SCD1 inhibition and sought to identify an appropriate model. Because high SCD1 expression was observed in many human cancer specimens, a panel of primary human cancer xenografts was evaluated to identify an appropriate *in vivo* model. A poorly differentiated gastric carcinoma model, GA16 (3+ for SCD1), was chosen because it shows relatively strong and uniform protein expression throughout the tumor cells in the xenograft (Fig. 5A). Two groups of mice bearing subcutaneous GA16 tumors were treated twice daily with 100 mg/kg A939572 or

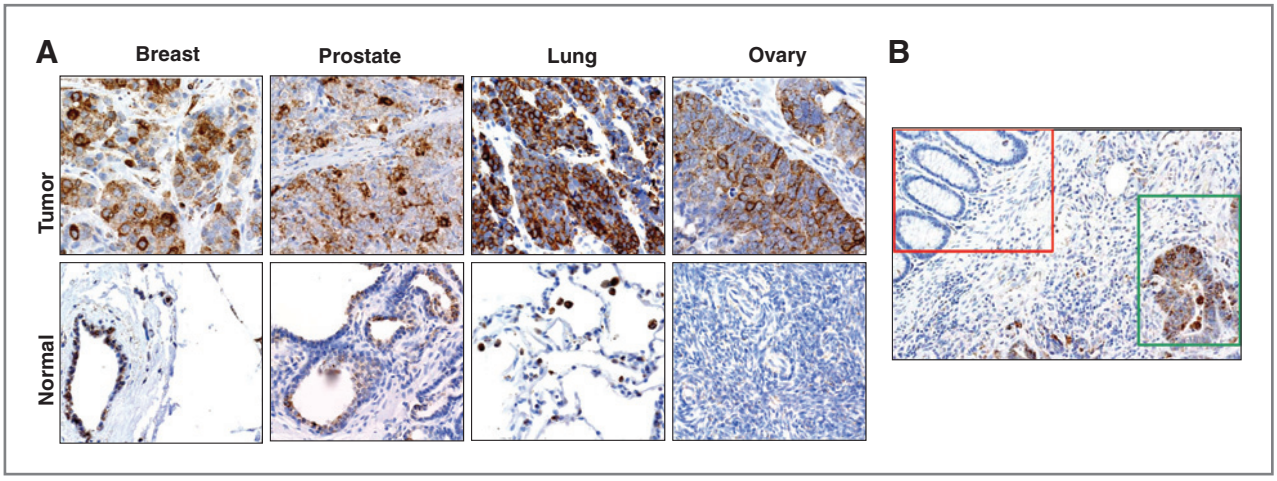

Figure 4. Immunohistochemical evidence that SCD1 is highly expressed in a large number of human cancers from various histologies. A, representative photomicrographs of positively staining tissue from breast (2+), prostate (2+), lung (3+), and ovarian (2+) cancer specimens as well as the respective normal tissues for each histology. B, an example of SCD1 immunostaining in a core taken from a colon cancer patient that contains negatively staining normal colon epithelial tissue (red box) and positively staining colon cancer tissue (green box).

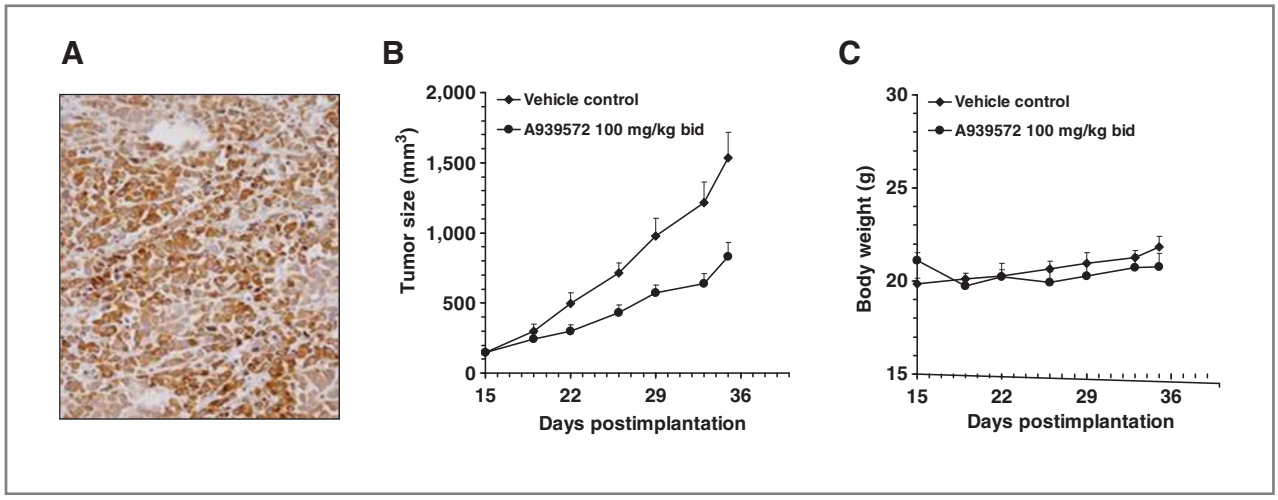

Figure 5. Pharmacologic inhibition of SCD1 suppresses tumor growth *in vivo*. A primary human gastric cancer xenograft (GA16. passage 6) was selected for evaluation of the antitumor effects of A939572 because of the high expression of SCD1 protein as determined by IHC (A). Mice bearing GA16 tumors with an average volume of 150 mm^3 were treated with vehicle or 100 mg/kg A939572 twice daily for 21 days. GA16 tumor growth was delayed by treating mice with A939572 (B), although no effect on body weight was observed (C).

an equal volume of the dosing vehicle. Administration of A939572 began when tumors reached an average target size of 150 mm^3 and continued for 21 days. Using this dose and schedule, serum concentrations of A939572 were maintained above 2 μmol/L (trough concentration) throughout the dosing regimen (data not shown). Within 7 days, a significant difference in tumor size was observed between A939572-treated and vehicle-treated groups. This trend continued throughout the dosing period (Fig. 5B). Following 21 days of dosing, the mean tumor volume in the A939572-treated group was reduced by nearly 50% relative to vehicle-treated animals. Throughout the study, animal weights were recorded and no significant changes in body weights were observed between A939572-treated and vehicle-treated animals (Fig. 5C). A939572 has been previously reported to cause potent reduction in oleic acid to stearic acid ratios in both liver and plasma samples from mice treated with a single dose of 10 mg/kg (19), 10-fold lower than the dose used in this study.

Discussion

Lipids play important roles in many cellular processes including membrane synthesis, energy storage, and cell signaling. Each of these processes is critical for the proliferation and survival of tumor cells. The composition of the lipids available for carrying out processes such as membrane biogenesis and lipid-mediated signaling is determined by the availability of the lipids and their precursors from the extracellular space, combined with the capacity of the cell to carry out *de novo* lipid synthesis and modification. The synthetic pathways for the creation of specialized lipid molecules are highly complex and utilize numerous enzymes with unique functions.

SCD1 is a widely studied enzyme that carries out a critical step in the production of MUFAs from SFA precursors. SFA and MUFA are the most abundant fatty acids in mammalian cells, and the ratio of SFA to MUFA can affect membrane fluidity and the activity of membrane associated receptors and enzymes (23, 24).

A growing body of evidence has recently emerged implicating the expression and activity of SCD1 in the proliferation and survival of cancer cells (4–14). We sought to understand whether pharmacologic inhibition of SCD1 might have therapeutic benefit in human cancers. Morgan-Lappe and colleagues (12) initially reported pronounced reduction in the viability of H1299 cells by RNAi-mediated SCD1 depletion. According to that report, H1299 cells were sensitive to the effects of SCD1 depletion while cultured in media containing 10% FBS. In our studies, however, sensitivity to SCD1 depletion was observed only when cells were cultured in reduced serum. The reason for the apparent discordance between our observations and those reported by Morgan-Lappe and colleagues (12) is not clear. It is possible that there may be a significant variability in composition of FBS from commercial suppliers. Nevertheless, we confirmed a striking effect of SCD1 depletion in cells cultured under reduced serum conditions.

Overall, excellent correlation was observed between the extent of protein depletion and the strength of the phenotypes observed. The loss of viability observed in siRNA-treated cells may be attributed to loss of SCD1 enzymatic function, as small molecule inhibition of SCD1 yielded a similar antiproliferative effect as SCD1 depletion.

As SCD1 is the rate-limiting enzyme required for the *de novo* production of MUFAs, we examined whether abundance of serum-derived lipids may be responsible for the differential effects of serum content on SCD1 levels and cell sensitivity to SCD1 inhibition. The results presented here provide evidence that SCD1 is induced by cells when exogenous mono- or polyunsaturated fatty acids are present in limited quantities, and we hypothesize that tumor cells

preferentially utilize exogenous unsaturated fatty acids available from the culture media or tumor microenvironment, until they become limiting. Once this occurs, SCD1 is induced to enable endogenous biogenesis of unsaturated fatty acids. We also show that supplementation of SFAs has no effect on the response of cells to SCD1 inhibition, further supporting the notion that cells treated with SCD1 inhibitors under conditions of limiting unsaturated fatty acids are growth inhibited due to lack of unsaturated fatty acids rather than buildup of excess SFAs. Overall, these data provide strong evidence that the availability of exogenous unsaturated fatty acids dictates sensitivity to SCD1 inhibition and that induction of SCD1 by cells predicts their dependence upon its enzymatic activity.

Although our results suggest that tumor cells require unsaturated fatty acids for survival, the ultimate reason for the dependence is not clear. Unsaturated fatty acids are important precursors for various products in the cell, including phospholipids (cell membrane), triglycerides (energy storage), and diacylglycerols (signaling), to name a few. It is possible that alterations in the fatty acid composition of any one of these molecules could affect cell function and, ultimately, survival. Expression profiling analyses of the cellular reaction to SCD1 inhibition revealed that many of the regulated transcripts are markers of the integrated stress/unfolded protein response, which occurs under conditions that cause ER stress (25). The ER is a major site of protein folding in the cell and is very sensitive to conditions that cause accumulation of unfolded proteins. These conditions cause signaling through PERK, IRE1, and ATF6, resulting in inhibition of protein translation and transcriptional activation of genes specifically involved in resolving ER stress. If the ER stress is rapidly resolved, signaling through PERK, IRE1, and ATF6 is interrupted and the process is reversed. Failure to resolve ER stress drives cells to undergo apoptosis (25, 26). Data have recently emerged showing that an excess of SFAs and cholesterol induces ER stress (27–29). In addition, Pineau and colleagues reported that ER stress induced by SFAs and sterols could be rescued by 4-phenyl butyrate, a molecular protein-folding chaperone (30). Furthermore, it has been shown that membrane sterols (which can themselves induce ER stress) inhibit protein translocation across the ER membrane (31). Our findings are consistent with those reported recently by Minville-Walz and colleagues showing that cell death induced by SCD1 depletion occurred via a CHOP-dependent mechanism (32). Because SCD1 is a resident ER protein, it is intriguing to hypothesize that SCD1 inhibition under conditions of limiting extracellular unsaturated fatty acids or excessive SFAs disrupts lipid homeostasis in the ER membrane, resulting in ER stress and, ultimately, apoptotic cell death.

Interestingly, ER stress response genes were also found to be differentially regulated in the livers of SCD1 knockout mice fed a very low-fat diet when compared with wild-type animals (33). The striking parallel in transcriptional alterations occurring in SCD1-deficient mice fed a very low-fat diet and tumor cells exposed to an SCD1 inhibitor under low-serum conditions further supports the notion that the availability of exogenous unsaturated lipids is responsible for the differential effects of SCD1 inhibition in varying serum concentrations. Another interesting parallel to the data presented here is that in mice maintained on a very low-fat diet, SCD1 mRNA is highly induced (34).

The results presented here strongly suggest that tumor cells require unsaturated fatty acids for survival. In the absence of an exogenous source, tumor cells induce SCD1 expression to allow endogenous lipid desaturation to occur. Under these conditions, SCD1 depletion or pharmacologic inhibition results in cell death via a mechanism involving ER stress. Furthermore, elevated SCD1 protein level strongly predicts sensitivity to SCD1 inhibition. The data presented here show, for the first time, that high SCD1 protein expression occurs in a large percentage of human cancers from various tissue origins. Given the prevalence of SCD1 overexpression in human cancer specimens, along with the strong correlation between SCD1 expression level and sensitivity to SCD1 inhibition *in vitro*, it seemed plausible to hypothesize that certain human cancers overexpressing SCD1 might be dependent upon SCD1 for growth and survival.

Our *in vivo* antitumor efficacy study shows that tumor growth inhibition can be achieved by pharmacologic inhibition SCD1 without causing any noticeable adverse effects in mice. These data provide strong evidence in support of SCD1 as a potentially viable target for the design of novel anticancer agents. Because SCD1 expression can be detected in many primary tumors and primary xenografts, additional testing will need to be carried out to thoroughly evaluate the antitumor activity of SCD1 inhibitors and the utility of SCD1 expression as a predictive biomarker for sensitivity to SCD1 inhibition.

Disclosure of Potential Conflicts of Interest

All authors are employees of Bristol-Myers Squibb Company.

The costs of publication of this article were defrayed in part by the payment of page charges. This article must therefore be hereby marked *advertisement* in accordance with 18 U.S.C. Section 1734 solely to indicate this fact.

Received March 16, 2011; revised August 8, 2011; accepted September 14, 2011; published OnlineFirst September 27, 2011.

References

1. Enoch HG, Catala A, Strittmatter P. Mechanism of rat liver microsomal stearyl-CoA desaturase. Studies of the substrate specificity, enzyme-substrate interactions, and the function of lipid. J Biol Chem 1976;251:5095–103.
2. Paton CM, Ntambi JM. Biochemical and physiological function of stearoyl-CoA desaturase. Am J Physiol Endocrinol Metab 2009;297:E28–37.
3. Wang J, Yu L, Schmidt RE, Su C, Huang X, Gould K, et al. Characterization of HSCD5, a novel human stearoyl-CoA desaturase unique to primates. Biochem Biophys Res Commun 2005;332:735–42.
4. Igal RA. Stearoyl-CoA desaturase-1: a novel key player in the mechanisms of cell proliferation, programmed cell death and transformation to cancer. Carcinogenesis 2010;31:1509–15.

5. Li J, Ding SF, Habib NA, Fermor BF, Wood CB, Gilmour RS. Partial characterization of a cDNA for human stearoyl-CoA desaturase and changes in its mRNA expression in some normal and malignant tissues. Int J Cancer 1994;57:348–52.
6. Falvella FS, Pascale RM, Gariboldi M, Manenti G, De Miglio MR, Simile MM, et al. Stearoyl-CoA desaturase 1 (Scd1) gene overexpression is associated with genetic predisposition to hepatocarcinogenesis in mice and rats. Carcinogenesis 2002;23:1933–6.
7. Scaglia N, Caviglia JM, Igal RA. High stearoyl-CoA desaturase protein and activity levels in simian virus 40 transformed-human lung fibroblasts. Biochim Biophys Acta 2005;1687:141–51.
8. Scaglia N, Igal RA. Stearoyl-CoA desaturase is involved in the control of proliferation, anchorage-independent growth, and survival in human transformed cells. J Biol Chem 2005;280:25339–49.
9. Maeda M, Scaglia N, Igal RA. Regulation of fatty acid synthesis and Delta9-desaturation in senescence of human fibroblasts. Life Sci 2009;84:119–24.
10. Scaglia N, Igal RA. Inhibition of stearoyl-CoA desaturase 1 expression in human lung adenocarcinoma cells impairs tumorigenesis. Int J Oncol 2008;33:839–50.
11. Scaglia N, Chisholm JW, Igal RA. Inhibition of stearoylCoA desaturase-1 inactivates acetyl-CoA carboxylase and impairs proliferation in cancer cells: role of AMPK. PLoS One 2009;4:e6812.
12. Morgan-Lappe SE, Tucker LA, Huang X, Zhang Q, Sarthy AV, Zakula D, et al. Identification of Ras-related nuclear protein, targeting protein for xenopus kinesin-like protein 2, and stearoyl-CoA desaturase 1 as promising cancer targets from an RNAi-based screen. Cancer Res 2007;67:4390–8.
13. Fritz V, Benfodda Z, Rodier G, Henriquet C, Iborra F, Avancès C, et al. Abrogation of *de novo* lipogenesis by stearoyl-CoA desaturase 1 inhibition interferes with oncogenic signaling and blocks prostate cancer progression in mice. Mol Cancer Ther 2010;9:1740–54.
14. Hess D, Chisholm JW, Igal RA. Inhibition of stearoylCoA desaturase activity blocks cell cycle progression and induces programmed cell death in lung cancer cells. PLoS One 2010;5:e11394.
15. Strebel K, Beck E, Strohmaier K, Schaller H. Characterization of foot-and-mouth disease virus gene products with antisera against bacterially synthesized fusion proteins. J Virol 1986;57:983–91.
16. Li X, Darzynkiewicz Z. Cleavage of poly(ADP-ribose) polymerase measured *in situ* in individual cells: relationship to DNA fragmentation and cell cycle position during apoptosis. Exp Cell Res 2000;255:125–32.
17. Obukowicz MG, Raz A, Pyla PD, Rico JG, Wendling JM, Needleman P. Identification and characterization of a novel delta6/delta5 fatty acid desaturase inhibitor as a potential anti-inflammatory agent. Biochem Pharmacol 1998;55:1045–58.
18. Dillon R, Greig MJ, Bhat BG. Development of a novel LC/MS method to quantitate cellular stearoyl-CoA desaturase activity. Anal Chim Acta 2008;627:99–104.
19. Xin Z, Zhao H, Serby MD, Liu B, Xin Z, Zhao H, et al. Discovery of piperidine-aryl urea-based stearoyl-CoA desaturase 1 inhibitors. Bioorg Med Chem lett 2008;18:4298–302.
20. Liu G, Lynch JK, Freeman J, Liu B, Xin Z, Zhao H, et al. Discovery of potent, selective, orally bioavailable stearoyl-CoA desaturase 1 inhibitors. J Med Chem 2007;50:3086–100.
21. Zhao H, Serby MD, Smith HT, Cao N, Suhar TS, Surowy TK, et al. Discovery of 1-(4-phenoxypiperidin-1-yl)-2-arylaminoethanone stearoyl-CoA desaturase 1 inhibitors. Bioorg Med Chem lett 2007;17:3388–91.
22. Oyadomari S, Mori M. Roles of CHOP/GADD153 in endoplasmic reticulum stress. Cell Death Differ 2004;11:381–9.
23. Stubbs CD, Smith AD. The modification of mammalian membrane polyunsaturated fatty acid composition in relation to membrane fluidity and function. Biochim Biophys Acta 1984;779:89–137.
24. Spector AA, Yorek MA. Membrane lipid composition and cellular function. J Lipid Res 1985;26:1015–35.
25. Szegezdi E, Logue SE, Gorman AM, Samali A. Mediators of endoplasmic reticulum stress-induced apoptosis. EMBO Rep 2006;7:880–5.
26. Lai E, Teodoro T, Volchuk A. Endoplasmic reticulum stress: signaling the unfolded protein response. Physiology (Bethesda) 2007;22:193–201.
27. Lai E, Bikopoulos G, Wheeler MB, Rozakis-Adcock M, Volchuk A. Differential activation of ER stress and apoptosis in response to chronically elevated free fatty acids in pancreatic beta-cells. Am J Physiol 2008;294:E540–50.
28. Laybutt DR, Preston AM, Akerfeldt MC, Kench JG, Busch AK, Biankin AV, et al. Endoplasmic reticulum stress contributes to beta cell apoptosis in type 2 diabetes. Diabetologia 2007;50:752–63.
29. Karaskov E, Scott C, Zhang L, Teodoro T, Ravazzola M, Volchuk A. Chronic palmitate but not oleate exposure induces endoplasmic reticulum stress, which may contribute to INS-1 pancreatic beta-cell apoptosis. Endocrinology 2006;147:3398–407.
30. Pineau L, Colas J, Dupont S, Beney L, Fleurat-Lessard P, Berjeaud JM, et al. Lipid-induced ER stress: synergistic effects of sterols and saturated fatty acids. Traffic 2009;10:673–90.
31. Nilsson I, Ohvo-Rekila H, Slotte JP, Johnson AE, von Heijne G. Inhibition of protein translocation across the endoplasmic reticulum membrane by sterols. J Biol Chem 2001;276:41748–54.
32. Minville-Walz M, Pierre A, Pichon L, Bellenger S, Fèvre C, Bellenger J, et al. Inhibition of stearoyl-CoA desaturase 1 expression induces CHOP-dependent cell death in human cancer cells. PLoS One 2010;5:e14363.
33. Flowers MT, Keller MP, Choi Y, Lan H, Kendziorski C, Ntambi JM, et al. Liver gene expression analysis reveals endoplasmic reticulum stress and metabolic dysfunction in SCD1-deficient mice fed a very low-fat diet. Physiol Genomics 2008;33:361–72.
34. Ntambi JM. Dietary regulation of stearoyl-CoA desaturase 1 gene expression in mouse liver. J Biol Chem 1992;267:10925–30.
35. Ohoka N, Yoshii S, Hattori T, Onozaki K, Hayashi H. TRB3, a novel ER stress-inducible gene, is induced via ATF4-CHOP pathway and is involved in cell death. EMBO J 2005;24:1243–55.
36. Whitney ML, Jefferson LS, Kimball SR. ATF4 is necessary and sufficient for ER stress-induced upregulation of REDD1 expression. Biochem Biophys Res Commun 2009;379:451–5.
37. Jiang HY, Wek SA, McGrath BC, Lu D, Hai T, Harding HP, et al. Activating transcription factor 3 is integral to the eukaryotic initiation factor 2 kinase stress response. Mol Cell Biol 2004;24:1365–77.
38. Lewerenz J, Maher P. Basal levels of eIF2alpha phosphorylation determine cellular antioxidant status by regulating ATF4 and xCT expression. J Biol Chem 2009;284:1106–15.
39. Hori O, Ichinoda F, Yamaguchi A, Tamatani T, Taniguchi M, Koyama Y, et al. Role of Herp in the endoplasmic reticulum stress response. Genes Cells 2004;9:457–69.
40. Gjymishka A, Su N, Kilberg MS. Transcriptional induction of the human asparagine synthetase gene during the unfolded protein response does not require the ATF6 and IRE1/XBP1 arms of the pathway. Biochem J 2009;417:695–703.
41. Ito D, Walker JR, Thompson CS, Moroz I, Lin W, Veselits ML, et al. Characterization of stanniocalcin 2, a novel target of the mammalian unfolded protein response with cytoprotective properties. Mol Cell Biol 2004;24:9456–69.
42. Wang M, Ye R, Barron E, Baumeister P, Mao C, Luo S, et al. Essential role of the unfolded protein response regulator GRP78/BiP in protection from neuronal apoptosis. Cell Death Differ 2010;17:488–98.